PHYSICAL REVIEW B VOLUME 57, NUMBER 2 1 JANUARY 1998-II

Dynamics of time-reversal-symmetry-breaking vortices in unconventional superconductors

Z. D. Wang
Department of Physics, University of Hong Kong, Pokfulam Road, Hong Kong, China

Qiang-Hua Wang
Department of Physics and National Laboratory of Solid State Microstructure, Nanjing University, Nanjing 210093 China and Department of Physics, University of Hong Kong, Pokfulam Road, Hong Kong, China

(Received 11 August 1997; revised manuscript received 20 October 1997)

Based on a two-component Ginzburg-Landau theory, we find a number of interesting behaviors of vortex dynamics in the time-reversal-symmetry-breaking (T-breaking) regime of the parameter space: (i) Only one of the two types of T-breaking vortices is stable against applied currents at intermediate and high fields; (ii) For these dynamically stable vortices, the equilibrium phase transitions at the lower and/or the upper critical fields may be of first order; (iii) The free vortex flow resistivity of the T-breaking vortices is generally nonlinear, and in the case of (ii) there are resistivity discontinuities at the first-order transitions. The phase diagram of the T-breaking vortices is presented. [S0163-1829(98)51302-1]

In recent years there have been extensive investigations on possible superconducting states arising from Cooper pairs with unusual (i.e., nonzero) angular momentum l. These activities were initiated by the discovery of superconductivity in some heavy-fermion superconductors,[1] high-T_c copper oxides,[2] and more recently in Ru-based layered perovskites with or without copper planes.[3] These materials share a common nature in the fact that all of them are systems of strongly correlated f- or d-shell electrons. It was argued, using the picture of the Bardeen-Cooper-Shrieffer theory of superconductivity, that these quasiparticles with f or d characters would have difficulty forming ordinary s-wave Cooper pairs due to the strong Coulomb repulsion. To avoid a large overlap of the wave functions of the paired particles, the system would rather choose an anisotropic channel, like a p-wave spin triplet or a d-wave spin singlet state, to form pairs. The nonzero angular momentum states lead to anisotropic energy gaps in the momentum space and thus to power law temperature dependencies in the specific heat, nuclear magnetic resonance and ultrasonic attenuation. The bulk magnetic properties may or may not be different from that in usual superconductors. From group theoretical methods, one can construct an appropriate Ginzburg-Landau (GL) theory for the possible superconducting states.[4–6] The GL theory is n-component depending on the number n of independent order parameters. It is clear that any one-component GL theory, irrespectively of the underlying pairing symmetry (or the angular momentum of the Cooper pair), is isomorphic to the conventional s-wave (or $l=0$) GL theory. Since the macroscopic properties predicted by one-component GL theories are generally not compatible with experiments, a number of authors have paid attention to many-component GL theories.[5] Numerical simulations performed for the two-component time-reversal-symmetry-breaking (T-breaking) superconductor [with a symmetry group $D_{6h}(\Gamma_5^{\pm})$] show that the system makes use of the possibility that each component can form its singularity spatially separated, and that the line energy of a vortex depends on the sign of its magnetic flux.[7] The difference in the line energy (and thus the lower critical field) is also accompanied by a certain difference in the vortex symmetry. More recently, our numerical simulations for a closely similar system reveal that in a certain region of the parameter space only one of the two types of T-breaking vortices is stable against applied currents and the free vortex flow resistivity may be highly nonlinear in a magnetic field. Following these trends, we consider *in the whole field region and parameter space* the equilibrium and *dynamic* properties of T-breaking vortices in the $D_{6h}(\Gamma_5^{\pm})$ system. Most importantly, several novel behaviors of vortex dynamics are found numerically.

The generic (Gibbs) GL free energy functional is identical for singlet and triplet pairing, and can be expressed as[5]

$$\begin{aligned} F=\int d\Omega & A(T)(|\eta_1|^2+|\eta_2|^2)+\beta_1(|\eta_1|^2+|\eta_2|^2)^2 \\ & +\beta_2(\eta_1^*\eta_2-\eta_1\eta_2^*)^2+K_1(|D_x\eta_1|^2+|D_y\eta_2|^2) \\ & +K_2(|D_x\eta_2|^2+|D_y\eta_1|^2)+K_3(D_x^*\eta_1^*D_y\eta_2+\text{c.c.}) \\ & +K_4(D_x^*\eta_2^*D_y\eta_1+\text{c.c.})+\frac{1}{8\pi}(\mathbf{B}-\mathbf{H})^2, \end{aligned} \tag{1}$$

where (η_1,η_2) are the two components of the order parameter in the real space, $\mathbf{D}=i\hbar\nabla-2e\mathbf{A}/c$, $\mathbf{B}=\nabla\times\mathbf{A}$ is the local magnetic induction, and $\mathbf{H}$ is the applied field. As usual, $A(T)\sim\ln T/T_c$ defines the superconducting transition temperature. The other coefficients are material dependent parameters. We note that the stiffness coefficients are mutually dependent as $K_1-K_2=K_3+K_4$ in the D_{6h} system. We shall be interested in the case where T-breaking may be realized. This occurs for such $\{\beta_i\}$ that $\beta_1>\beta_2>0$. The T-breaking two-fold degenerated bulk phases are $(\eta_1,\eta_2)=\eta_0(1,\pm i)$ with $|\eta_0|^2=-A(T)/4(\beta_1-\beta_2)$. Following the convention, we define $\mathbf{q}=i\eta\times\eta^*/|\eta|^2$, which can be nonzero only if time-reversal symmetry is broken, i.e., η cannot be transformed to η^* by any simple gauge transform. Furthermore, define $\eta_{\pm}=(\eta_1\pm i\eta_2)/\sqrt{2}|\eta_0|$.

Then $\mathbf{q}=(|\eta_-|^2-|\eta_+|^2)\hat{z}$. The two pure T-breaking phases are the η_+ phase (with $q=-1$) and the η_- phase (with $q=1$). In the context of singlet (triplet) pairing, q is proportional to the z-axis projection of the internal angular momentum (pseudospin) of the Cooper pair.[5,7] In the presence of a magnetic field, both T-breaking phases could appear with one of them dominating the other. It was found that there exist two classes of T-breaking vortices in the D_{6h} system: P (AP) vortex stabilized when the applied magnetic field $\mathbf{H}$ is parallel (antiparallel) to $\mathbf{q}$ of the dominant phase.[7–9] For later use let us define $\beta=\beta_2/4(\beta_1-\beta_2)$, $k_i=K_i/(K_1+K_2)$, $k=(k_3+k_4)/2$, $\Delta k=(k_3-k_4)/2$, and $\kappa=\lambda/\xi$ with $\lambda^{-2}=8\pi(2e)(K_1+K_2)|\eta_0|^2/c$ and $\xi^2=-(K_1+K_2)/2A(T)$. Then in the present system the control parameters are β, k, Δk and κ.[10] (Notice that $k_1+k_2=1$ and $k_1-k_2=2k$.) Normalizing the space and the vector potential by ξ and $A_0=\Phi_0/2\pi\xi$, respectively, the dimensionless free energy $f=F/(H_c^2\xi^2/4\pi)$ ($H_c=\Phi_0/2\sqrt{2}\pi\xi\lambda$ being the thermodynamic critical field) can be cast into

$$
\begin{aligned}
f=\int d\Omega &- \tfrac{1}{2}(|\eta_+|^2+|\eta_-|^2)+\tfrac{1}{8}(|\eta_+|^2+|\eta_-|^2)^2 \\
&+2\beta|\eta_+|^2|\eta_-|^2+(\tfrac{1}{2}-\Delta k)(|\pi_+\eta_+|^2+|\pi_-\eta_-|^2) \\
&+(\tfrac{1}{2}+\Delta k)(|\pi_-\eta_+|^2+|\pi_+\eta_-|^2) \\
&+2k[(\pi_+\eta_-)^*\pi_-\eta_+ + \text{c.c}]+\kappa^2(\mathbf{b}-\mathbf{h})^2,
\end{aligned}
$$

where $\pi_\pm=d_x\pm id_y$ with $d_{x,y}=i\partial_{x,y}-a_{x,y}$. Here $a_{x,y}=A_{x,y}/A_0$, $\mathbf{b}=\nabla\times\mathbf{a}=\mathbf{B}/B_0$ and $\mathbf{h}=\mathbf{H}/B_0$ with $B_0=A_0/\xi=\Phi_0/2\pi\xi^2$. The operators $\pi_\pm$ satisfy the bosonic-like commutation relation $[\pi_+,\pi_-]=b$. It is seen that Δk-term is diagonal in the ''bosonic'' occupation space and is equivalent to the Zeeman splitting, while the k term is off-diagonal. Obviously the system can gain energy by mixing the two phases $\eta_\pm$ in a suitable way due to the Δk and k terms. On the other hand, the β term is seen to be repulsive for the two phases if $\beta>0$. Thus nonaxial T-breaking vortex states would arise from a mixture of both phases below a critical value of β, namely, $0<\beta\leq\beta_c$, where $\beta_c\sim0.058$.[7] The weak coupling limit would give $k=1/4$ and $\Delta k=0$. Strong correlation effects would yield much more complicated situations. Although there exists no microscopic theoretical justification, we assume reasonably that $k_1>0$ and $k_2>0$. Then $-1/2\leq k\leq 1/2$. By symmetry, it suffices to consider the range $0\leq k\leq 1/2$.

To proceed, we fix $\beta=0.02$ and $\kappa=2$ since closely similar results are found for other values of $\beta\leq\beta_c$ and $\kappa>2$. For definiteness we shall fix the direction of $\mathbf{H}$ along the high symmetry axis (z axis) of the D_{6h} system with $H>0$. The upper critical field for the present system can be obtained from the linearized GL equations: $H_{c2}^I=B_0/(1-2\Delta k)$ or $H_{c2}^{II}=B_0/[3-2\sqrt{(1-\Delta k)^2+8k^2}\,]$, with the larger one as the relevant critical field H_{c2}.[5,7] Moreover, near the critical field, the vortices would be locally axial (or nonaxial) if $H_{c2}=H_{c2}^I$ (or H_{c2}^{II}).[5,7] Assuming pure dissipative dynamics, the time-dependent GL equations are simply obtained as $\partial_t u=-\Gamma\,\delta f/\delta u^*$ for $u=\eta_+$ and η_-, and $\partial_t\mathbf{a}=-\Gamma\,\delta f/\delta\mathbf{a}$ where a dimensionless applied current $\mathbf{j}$ can be included by requiring $\nabla\times\mathbf{h}=\mathbf{j}$. In these time-dependent GL equations,

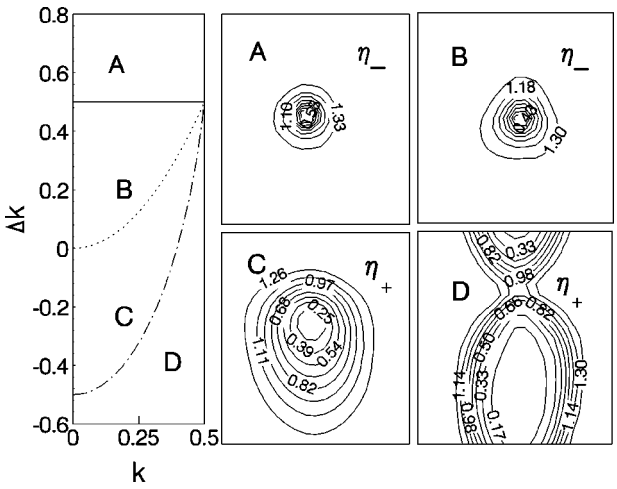

FIG. 1. Left panel: Phase diagram of the T-breaking vortices in the k-Δk parameter space. Middle and right panels: schematic profile of the dominant phase ($\eta_\pm$) for a single vortex in the corresponding parameter region.

we have chosen a gauge in which the electrostatic potential does not appear so that the electric field (and thus the resistivity) can be obtained as $\mathbf{E}=-\partial_t\mathbf{A}$. The dissipation parameter Γ is chosen in such a way that the dimensionless resistivity in the normal state is unity. The technical details of the simulations of the vortex states have been described elsewhere.[9,11] An important finding in our simulations is the fact that even though the two types of T-breaking vortices can be stabilized at low fields in the equilibrium state,[7] generally only one type of them, either the P-type or the AP-type vortices, remains stable against an applied current at higher fields provided that $H_{c2}^I\neq H_{c2}^{II}$. Therefore, we shall limit ourselves to these *dynamically stable* T-breaking states.

The phase diagram in the k-Δk parameter space for the vortex states is depicted schematically in Fig. 1 (left panel). The T-violating vortices are stabilized in the four regions A, B, C, and D. In region A (D) only H_{c2}^{II} (H_{c2}^I) is well defined. In region B (C) both critical fields are defined with $H_{c2}^I>H_{c2}^{II}$ ($H_{c2}^I<H_{c2}^{II}$). Along the dashed line $\Delta k=2k^2$ separating regions B and C, one has $H_{c2}^I=H_{c2}^{II}$. We skip the range $|\Delta k|>1$ where the system would be generally unstable. Schematic contour drawings of $|\eta_\pm|$ for a single vortex at low fields are presented in the middle and right $10\xi\times10\xi$ panels of Fig. 1 for each parameter regime. The behaviors of the T-breaking vortices in the four regions are described in alphabetical order in the following.

The dynamically stable vortices are P-type vortices in region A. The dominant phase is η_- with a local axial symmetry at the core region (see Fig. 1). The ambient phase η_+ is peaked and localized at the core edge of η_-, sharing one singularity point with η_-. For $k=0.4$ and $\Delta k=0.6$ we observed that $|\eta_-|_{\max}\sim1.4$ and $|\eta_+|_{\max}\sim0.26$. The Gibbs free energy density is shown in Fig. 2(a), from which we read off $H_{c1}\approx0.124B_0$ from the intersection of Meissner-state line (solid) and the mixed-state line, and $H_{c2}\sim1.04B_0$ from the intersection of the mixed-state line (open circles) and the normal-state line (dashed). Astonishingly, $H_{c2}<H_{c2}^{II}=5/3B_0$. In fact, although the mixed state and the normal state intersect at $H=H_{c2}$, the amplitudes of the order

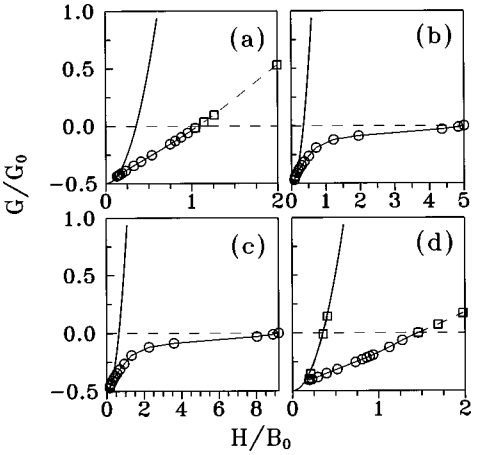

FIG. 2. Gibbs free energy density as a function of applied field. Here $k=0.4$, and $\Delta k=0.6$, 0.4, 0.1, and -0.1 in (a), (b), (c) and (d), respectively. Open squares indicate metastable states. Here $G_0=H_c^2/4\pi$.

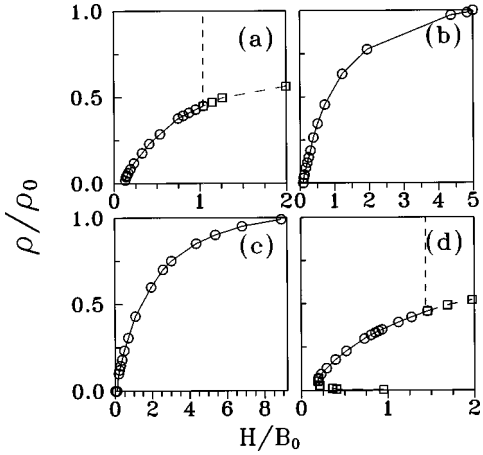

FIG. 4. Free vortex flow resistivity as a function of applied field corresponding to Fig. 2. Open squares indicate metastable states. Vertical dashed lines indicate resistivity jump at the first-order phase transitions.

parameters do not decrease to zero at all. The mixed state at $H>H_{c2}$ is metastable. This clearly demonstrates that there is a *first-order* phase transition at H_{c2}, instead of the usual second-order one. As a further strong test of the reliability of H_{c2} determined above, we plot the magnetization curve in Fig. 3(a) to find that the sum-rule-like thermodynamic identity $-4\pi\int_0^{H_{c2}}M\,dH=H_c^2/8\pi$ (sum rule hereafter) is satisfied excellently. Here $H_c^2/8\pi$ is the condensation energy density at zero field. Furthermore, the magnetization jump $\Delta M\sim 0.06B_0/4\pi$ at H_{c2} is obvious. Another important aspect of the vortex dynamics is the vortex flow resistivity as a function of magnetic field, which we present in Fig. 4(a), where we see two anomalies immediately. First, the free vortex flow resistivity ρ_F is nonlinear at $H\leqslant H_{c2}$. Second, there is a sizable resistivity jump, $\Delta\rho/\rho_n\sim 0.55$ at $H=H_{c2}$, beyond which the system enters the normal state. While the magnetization drop might be too small to be observable, the resistivity jump is large enough for experimental measurements.

The P vortices are also dynamically stable in region B. However, in the low-field region, a single P vortex has a local symmetry of a triangle in the core region (see, e.g., Ref. (7) and Fig. 1). At higher fields, the core of the dominant η_- phase undergoes a transition to be locally axial while the ambient η_+ phase becomes fourfold symmetric locally and decreases its amplitude continuously to zero at $H=H_{c2}$ where the amplitude of η_- also goes to zero continuously. For $k=\Delta k=0.4$ we have $H_{c2}=5B_0$ (with $H_{c2}^I=5B_0$ and $H_{c2}^{II}=2.2792B_0$). The Gibbs free energy density as a function of the field in this case is shown in Fig. 2(b), which seems usual at a first sight. However, the lower critical field read off from Fig. 2(b) is roughly $H_{c1}\sim 0.09$, which is almost two orders of magnitude smaller than H_{c2}. Evidently, the effective GL parameter $\kappa_{\rm eff}\gg\kappa=2$. The magnetization curve is shown in Fig. 3(b). The sum rule is also checked to be satisfied within numerical uncertainties. The value of $|4\pi M|$ is extremely low in a large portion of the field range. These features show that such superconductors are more easily subject to field penetration. Nevertheless, the field-driven transitions at $H=H_{c1}$ and H_{c2} are both of the usual second order. The free vortex flow resistivity in the present case, as shown in Fig. 4(b), is highly nonlinear with a downward curvature. The characteristic crossover in the resistivity is reminiscent of the core transition of the dominant η_- phase. We suggest that two essentially different dissipation mechanisms may be operating respectively at low and high fields, and the nonlinear resistivity could be utilized to explain the anomalous B-T curve (defined by vanishing resistivity) observed by Wu *et al.* in a Ru-based perovskite.[3,9]

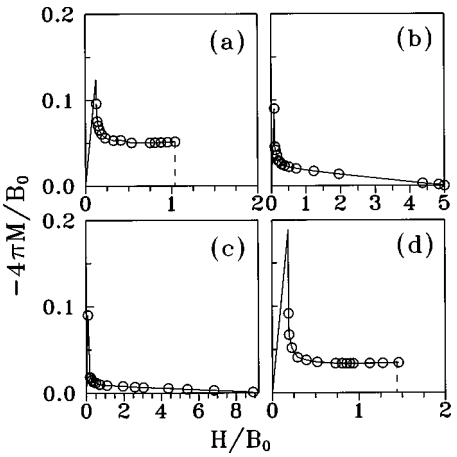

FIG. 3. Equilibrium magnetization curve corresponding to Fig. 2. The metastable states are skipped for clarity.

The properties of the vortices in region C of Fig. 1 are similar to those in region B, except that the dynamically stable T-breaking vortices are AP vortices. Near the lower critical field, a single vortex looks like a crescent (see middle panel C of Fig. 1). Higher fields drive a core transition as seen in region B of Fig. 1. For $k=0.4$ and $\Delta k=0.1$, the upper critical field is given by $H_{c2}=H_{c2}^{II}=9.205B_0$. The Gibbs free energy density, the equilibrium magnetization curve and the free vortex flow resistivity are shown in Figs. 2(c), 3(c), and 4(c), respectively. The lower critical field extracted from Figs. 2(c) and 3(c) is approximately $H_{c1}\sim 0.145B_0$. We have also examined the special case $H_{c2}^I=H_{c2}^{II}$ to find that the vortices are axially symmetric and

the flow resistivity is linear even though time-reversal-symmetry is broken. Combining Figs. 4(b) and 4(c) we conjecture that in the regions B and C of Fig. 1 the flow resistivity is generally nonlinear in an applied field.

Even more interesting magnetic properties are found in region D of Fig. 1, where the dynamically stable vortices are AP vortices. At low fields ($\sim H_{c1}$), the crescent-shaped AP vortices become unstable against expansion of the core region, so that the vortices are not spatially localized and mutually separated as the usual vortices and the vortices in the other regions of Fig. 1, but are connected by domain walls (see right panel D of Fig. 1). The amplitudes of the two phases η_+ and η_- just complement each other, signaling that the system is developing in such a way that either one of these phases would have prevailed in the whole space if there were no magnetic flux. That is, the vortex state at these low fields is metastable. This is indeed perceivable from the Gibbs free energy density presented in Fig. 2(d) for $k=0.4$ and $\Delta k=-0.1$: At the low-field side, if we decreased the average magnetic induction below a critical value $B_{c1}\neq 0$, the applied magnetic field extracted from the Virial theorem[12] would begin to *increase* so that the Gibbs free energy would cease to decrease, but would increase along a metastable path (open squares). (The reason why those metastable states are obtained is because of the periodic boundary condition with one flux quantum.) These states are, of course, unphysical. Rather, the system should be readily in the Meissner state. The lower critical field $H_{c1}\sim 0.1894B_0$ at $\overline{B}=B_{c1}=0.0897B_0$, in contrast to $B_{c1}=0$ in usual cases. The abrupt change in the vortex density (i.e., $\overline{B}$) around H_{c1} is clearly a first-order phase transition. Near and above the lower critical field, the magnetic-induction profile is nontrivial in that even though the average induction is positive, there are regions along the edge of the degrading crescent vortex, or the domain walls, where the local induction is positive or negative, of an amplitude of $\sim 0.15B_0$, in the two sides of the domain walls (not shown here). Such a violent magnetic induction fluctuation would be easily observed in neutron diffraction measurements. On the other hand, higher fields drive a core transition as in region C of Fig. 1. And the mixed state is stabilized up to $H=H_{c2}=1.460B_0$, beyond which the free energy of the mixed state is higher than the normal state, but the amplitude of the order parameters do not decrease at all. Thus another first-order field-driven phase transition occurs at H_{c2}. Surprisingly this upper critical field is substantially higher than $H_{c2}^{l}=0.8333B_0$. The values of H_{c1} and H_{c2} are compatible with the magnetization curve depicted in Fig. 3(d) in that the sum rule is satisfied. As a consequence of the first order transition, the magnetization has discontinuities at the critical fields H_{c1} and H_{c2}. Like that in Fig. 4(a), we see in Fig. 4(d) that the corresponding resistivity has jumps at the first order transition points at H_{c1} and H_{c2} (with the jump at H_{c1} being much smaller). More precisely, the flow resistivity is nonzero at H_{c1} because of a sudden penetration of a finite density of vortices, and it has not reached the normal-state resistivity just before the transition to the normal state.

[1] G. R. Stewart, Z. Fisk, J. O. Willis, and J. L. Smith, Phys. Rev. Lett. **52**, 679 (1984).

[2] J. G. Bednorz and K. A. Müller, Z. Phys. B **64**, 189 (1986).

[3] Y. Maeno, H. Hashimoto, K. Yoshida, S. Nishizaki, T. Fujita, J. G. Bednorz, and F. Lichtenberg, Nature (London) **372**, 532 (1994).

[4] G. E. Volovik and L. P. Gor'kov, Sov. Phys. JETP **61**, 843 (1985); M. Wu, D. Chen, F. Chien, S. Sheen, D. Ling, C. Tai, G. Tseng, D. Chen, and F. Zhang, Z. Phys. B **102**, 37 (1997).

[5] M. Sigrist and K. Ueda, Rev. Mod. Phys. **63**, 239 (1991), and references cited therein.

[6] M. Ozaki and K. Machida, J. Phys. Soc. Jpn. **61**, 1277 (1992).

[7] T. Tokuyasu, D. Hess, and J. Sauls, Phys. Rev. B **41**, 8891 (1990).

[8] K. Machida, T. Fujita, and T. Ohmi, J. Phys. Soc. Jpn. **62**, 680 (1993).

[9] Q.-H. Wang and Z. D. Wang (unpublished).

[10] Here κ plays a role similar to the GL parameter but it may be different from the actual effective one in the present case. λ and ξ are length scales similar to the London penetration depth and the coherence length, respectively.

[11] Q. Wang and Z. D. Wang, Phys. Rev. B **54**, R15 645 (1996); Z. D. Wang and Q.-H. Wang, *ibid.* **55**, 11 756 (1997).

[12] M. Doria, J. Gubernatis, and D. Rainer, Phys. Rev. B **39**, 9573 (1989); Z. D. Wang and C.-R. Hu, *ibid.* **44**, 11 918 (1991).